

Learning Gaussian Graphical Models with Ordered Weighted ℓ_1 Regularization

Cody Mazza-Anthony, Bogdan Mazoure, and Mark Coates, *Senior Member, IEEE*

Abstract—We address the task of estimating sparse structured precision matrices for multivariate Gaussian random variables within a graphical model framework. We propose two novel estimators based on the Ordered Weighted ℓ_1 (OWL) norm: 1) The Graphical OWL (GOWL) is a penalized likelihood method that applies the OWL norm to the lower triangle components of the precision matrix. 2) The column-by-column Graphical OWL (ccGOWL) estimates the precision matrix by performing OWL regularized linear regressions. Both methods can simultaneously identify groups of related edges in the graphical model and control the sparsity in the estimated precision matrix. We propose proximal descent algorithms to find the optimum for both estimators. For synthetic data where group structure is present, the ccGOWL estimator requires significantly reduced computation and achieves similar or greater accuracy than state-of-the-art estimators. Timing comparisons are presented and demonstrate the superior computational efficiency of the ccGOWL. We demonstrate the efficacy of the ccGOWL estimator on two domains—gene network analysis and econometrics.

Index Terms—Gaussian graphical models, precision matrix estimation, ordered weighted least squares, sparse estimation.

I. INTRODUCTION

The task of estimating highly modular structures based on relationships found in the data frequently arises in computational biology and finance [1]. Due to the large volume and high dimensionality of data in these disciplines, the speed of inference procedures and interpretability can be improved by leveraging the structured relations between inputs [2]. For example, it is often desirable to induce sparsity in an effort to reduce cross-pathway connections between genes when considering gene expression data.

Gaussian graphical models (GGMs) are well-suited for modeling conditional independence through the non-zero pattern of the inverse covariance matrix. From a probabilistic point of view, the precision (inverse covariance) matrix directly encodes the conditional independence relations between its elements. The most well-known algorithm for learning sparse GGMs is the *graphical lasso* [3], which imposes graph sparsity through maximization of an ℓ_1 -penalized Gaussian log-likelihood with block coordinate descent. Current state-of-the-art methods [4]–[7] also rely on ℓ_1 penalized structural

learning. However, estimating the precision matrix column-by-column has received considerable attention since such an approach can be numerically simpler and still achieve similar performance [8], [9].

Related work can be organized into three classes: 1. *Methods which learn a graph given groups a priori*: This class includes [7] which applies a group ℓ_1 penalty to encourage structured sparsity but requires a set of pre-defined hyperparameters to control the topology of the network. In other works, prior knowledge is used to assign edge weights in order to predict underlying group structure [10]–[13]. 2. *Methods which first find groups and then learn the structure within each group*: This class includes [5] which proposes a two-step approach to the problem, first applying hierarchical clustering to identify groups and then using the graphical lasso within each group. [14] detects groups in the covariance matrix using thresholding and then apply graphical lasso to each group. 3. *Methods which learn both group and graph structures simultaneously*: [6] uses a non-decreasing, concave penalty function to identify densely connected nodes in the network. [4] proposes the GRAB estimator that solves a joint optimization problem which alternates between estimating overlapping groups encoded into a Laplacian prior and learning the precision matrix. [15] proposes a framework for structured graph learning that imposes Laplacian spectral constraints. [16] applies a structured norm to precision matrix estimation to identify overlapping groups.

This paper presents two novel estimators for identifying the precision matrices associated with structured Gaussian graphical models and makes four major contributions. First, both estimators require only a small amount of *a priori* information and do not require any information about group structure. More specifically, they only require two hyperparameters (one for sparsity and one for grouping) when using the OSCAR-like weight generation procedure [17]. This differs from [7], which requires p^2 hyperparameters, and GRAB [4], which requires a more constrained objective accompanied by an additional hyperparameter for each constraint. Second, both estimators can learn network structure in a single-step proximal descent procedure. This is an advantage over the *cluster graphical lasso* [5], which solves the task with a two-step procedure by alternating between clustering and gradient steps. Likewise, the GRAB algorithm also alternates between learning the overlapping group prior matrix and learning the inverse covariance. Our focus is on estimating the graphical model, rather than identifying groups, but we can apply a Gaussian Mixture Model (GMM) or other clustering algorithms to identify overlapping groups from our precision matrix estimate.

This work was supported by the Department of National Defence's Innovation for Defence Excellence and Security (IDEaS) program. We acknowledge the support of the Natural Sciences and Engineering Research Council of Canada (NSERC), [2017-260250]. C. Mazza-Anthony and Mark Coates are with the Department of Electrical and Computer Engineering, McGill University, Montreal, QC, Canada. e-mails: cody.mazza-anthony@mail.mcgill.ca, mark.coates@mcgill.ca. B. Mazoure is with the School of Computer Science, McGill University, Montreal, QC, Canada. email: bogdan.mazoure@mail.mcgill.ca.

Third, we establish the uniqueness of the GOWL estimator by deriving its dual formulation. Fourth, the ccGOWL framework provides new theoretical guarantees for grouping related entries in the precision matrix and offers a more computationally efficient algorithm. When comparing ccGOWL to the previously mentioned penalized likelihood methods, it is clear that the ccGOWL estimator is more computationally attractive in the high dimensional setting as it can be obtained one column at a time by solving a simple linear regression that can be easily parallelized/distributed.

The proposed GOWL and ccGOWL estimators are based on a different notion of groups than the algorithms discussed above. Previous methods consider groups or blocks of *variables*. Structural priors then encourage group (block) sparsity — an edge in the graphical model (a non-zero precision matrix entry) is modelled as more likely if it connects variables that belong to the same group. In contrast, the GOWL estimator introduces a structural prior that encourages grouping of *edges* in the graphical model. The GOWL estimator favours precision matrix estimates where multiple entries have the same value, i.e., the pairs of variables are estimated to have the same partial correlation. The GOWL structural prior thus models scenarios where the relationships between multiple pairs of variables are likely to have the same strength, with the relationships arising from a common cause or being impacted by a common factor. As an example, consider three mining companies which focus on different metals; we might a priori expect the partial correlations between the stock prices and the specific metal prices to be of the same magnitude. The ccGOWL estimator is similar, but only encourages grouping of edges that have one variable in common. For this case, consider an example of a single company that devotes equal resources to mining three metals; we might model the partial correlations between the company's stock price and the three metals to be equal.

Figure 1 illustrates the relationship between the design matrix, precision matrix, and the resulting penalized GGM. GOWL penalizes certain groups of edges all together while ccGOWL penalizes edges for each node separately. The goal is to promote groups of related edges taking the same value while penalizing less relevant relationships between variables.

A. Notation and Preliminaries.

Throughout the paper, we highlight vectors and matrices by lowercase and uppercase boldfaced letters, respectively. For a vector $\mathbf{a} \in \mathbb{R}^p$, let \mathbf{a}_{-i} denote a vector with its i^{th} component removed. For a symmetric matrix $\mathbf{A} \in \mathbb{R}^{p \times p}$, $\mathbf{A}_{i,*}$ represents the i^{th} row of \mathbf{A} and $\mathbf{A}_{*,j}$ denotes the j^{th} column of \mathbf{A} , $\mathbf{A}_{i,-j}$ denotes the i^{th} row of \mathbf{A} with its j^{th} entry removed, $\mathbf{A}_{-i,j}$ denotes the j^{th} column of \mathbf{A} with its i^{th} entry removed, and the matrix $\mathbf{A}_{-i,-j}$ denotes a $(p-1) \times (p-1)$ matrix obtained by removing the i^{th} row and j^{th} column. Moreover, we denote as $\text{vechs}(\mathbf{A})$ the strict column-wise vectorization of the lower triangular component of \mathbf{A} :

$$\text{vechs}(\mathbf{A}) = [\mathbf{A}_{2,1}, \dots, \mathbf{A}_{n,1}, \mathbf{A}_{3,2}, \dots, \mathbf{A}_{n,2}, \mathbf{A}_{n,n-1}].$$

For a vector $\mathbf{a} = (a_1, \dots, a_p)^T \in \mathbb{R}^p$, we use the classical definition of the ℓ_q norm, that is $\|\mathbf{a}\|_q = (\sum_{i=1}^p |a_i|^q)^{1/q}$ for

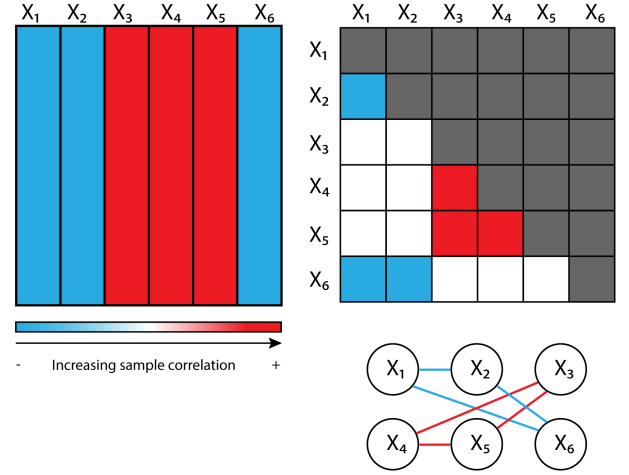


Fig. 1: A design matrix, precision matrix, and network with two groups of edges that share similar sample partial correlation.

$1 \leq q \leq \infty$. The i^{th} largest component in magnitude of the p -tuple $(|a_1|, |a_2|, \dots, |a_p|)$ is denoted $a_{[i]}$. The vector obtained by sorting (in non-increasing order) the components of \mathbf{a} is denoted $\mathbf{a}_{\downarrow} = (a_{[1]}, a_{[2]}, \dots, a_{[p]})$. For matrices and vectors, we define $|\cdot|$ to be the element-wise absolute value function.

II. BACKGROUND

A. Gaussian Graphical Models (GGM)

A GGM aims to determine the conditional independence relations of a set of random jointly Gaussian variables. Suppose $\mathbf{X} = [\mathbf{X}_1, \dots, \mathbf{X}_n]^T$, $\mathbf{X}_i \sim N(\mathbf{0}, \Sigma)$ is a collection of i.i.d. p -dimensional random samples. Assume that the columns of the design matrix \mathbf{X} have been standardized to have zero mean and unit variance. Let \mathbf{S} denote the (biased, maximum likelihood) sample covariance matrix, defined as $\mathbf{S} = n^{-1} \sum_{k=1}^n \mathbf{X}_k \mathbf{X}_k^T$ and let Θ denote the precision matrix, defined as $\Theta = \Sigma^{-1}$. It is well understood that the sparsity pattern of Θ encodes the pairwise partial correlation between variables. More specifically, the ij^{th} entry in Θ is zero if and only if variables i and j are conditionally independent given the remaining components [18], [19]. The GLASSO algorithm has been proposed to estimate the conditional independence graph embedded into Θ through ℓ_1 regularization of Gaussian maximum likelihood estimation:

$$\min_{\Theta \succ 0} -\log \det \Theta + \text{tr}(\mathbf{S}\Theta) + \lambda \|\Theta\|_1, \quad (1)$$

where λ is a nonnegative tuning parameter that controls the level of sparsity in Θ . Under the same assumptions, [9] showed that Θ can be estimated through column-by-column linear regressions. Letting $\mathbf{x}_j \sim N(\mathbf{0}, \Sigma)$ for $j = 1, \dots, n$, the conditional distribution of x_j given \mathbf{x}_{-j} satisfies:

$$x_j | \mathbf{x}_{-j} \sim N(\beta_j^T \mathbf{x}_{-j}, \sigma_j^2),$$

where $\beta_j = (\Sigma_{-j,-j})^{-1} \Sigma_{-j,j} \in \mathbb{R}^{p-1}$ and $\sigma_j^2 = \Sigma_{j,j} - \Sigma_{j,-j}(\Sigma_{-j,-j})^{-1} \Sigma_{-j,j}$. Thus, we can write the following

$$x_j = \beta_j^T \mathbf{x}_{-j} + \varepsilon_j,$$

where $\varepsilon_j \sim N(0, \sigma_j^2)$. By the block matrix inversion formula we define:

$$\Theta_{j,j} = \sigma_j^{-2}, \quad \text{and} \quad \Theta_{-j,j} = -\sigma_j^{-2} \beta_j.$$

Thus, we can estimate the precision matrix column-by-column by regressing x_j on \mathbf{x}_{-j} , and a LASSO procedure can be adopted by solving:

$$\hat{\beta}_j = \arg \min_{\beta_j \in \mathbb{R}^{p-1}} \|\mathbf{X}_{*,j} - \mathbf{X}_{*,-j} \beta_j\|_2^2 + \lambda \|\beta_j\|_1. \quad (2)$$

B. OWL in the Linear Model Setting

In the linear regression setting, much interest has been given to regularizers that can identify groups of highly correlated predictors. This is often referred to as *structured/group sparsity*. Regularization penalties targeting such structure include the *elastic net* [20], the *fused lasso* [21] and the recently proposed *order weighted ℓ_1 lasso* [22], [23]. Suppose that the response vector $\mathbf{y} \in \mathbb{R}^n$ is generated from a linear model of the form: $\mathbf{y} = \mathbf{X}\beta + \varepsilon$ where $\mathbf{X} \in \mathbb{R}^{n \times p}$ is the design matrix, $\beta \in \mathbb{R}^p$ is the vector of regression coefficients, $\mathbf{y} \in \mathbb{R}^n$ is the response vector, and $\varepsilon \in \mathbb{R}^n$ is a vector of zero-centered homoscedastic random errors distributed according to $\mathcal{N}(0, \sigma^2)$. The OWL regularizer is then defined to be:

$$\Omega_{\text{OWL}}(\beta) = \sum_{i=1}^p \xi_i |\beta|_{[i]}, \quad (3)$$

where $\beta_{[i]}$ is the i^{th} largest component in magnitude of $\beta \in \mathbb{R}^p$, and $\xi \in \mathbb{R}_+^p$. OSCAR [17] is a particular case of the OWL that consists of a combination of a ℓ_1 and a pairwise ℓ_∞ terms and in its original formulation is defined as

$$\lambda_1 \sum_{i=1}^p |\beta_i| + \lambda_2 \sum_{i < j} \max\{|\beta_i|, |\beta_j|\}. \quad (4)$$

The OSCAR weights can be recovered within OWL by setting $\xi_i = \lambda_1 + \lambda_2(p-i)$ where $\lambda_1 > 0$ controls the level of sparsity and $\lambda_2 > 0$ controls the degree of grouping. In [22], the OWL regularizer is referred to as *sorted ℓ_1 penalized estimation* (SLOPE).

C. Proximal Methods

Proximal algorithms form a class of robust methods which can help to solve composite optimization problems of the form:

$$\min_{x \in \mathcal{X}} g(x) + h(x), \quad (5)$$

where \mathcal{X} is a Hilbert space with associated inner product $\langle \cdot, \cdot \rangle$ and norm $\|\cdot\|$, and $g : \mathcal{X} \mapsto \mathbb{R}$ is a closed, continuously differentiable, and convex function. The function $h : \mathcal{X} \mapsto \mathbb{R}$ is a convex, not necessarily differentiable function. The *proximal mapping* of a convex function h , denoted by $\text{prox}_h : \mathcal{X} \rightarrow \mathcal{X}$, is given by

$$\text{prox}_h(v) = \arg \min_x \left(h(x) + \frac{1}{2} \|x - v\|_2^2 \right). \quad (6)$$

In general, this family of algorithms uses the proximal mapping to handle the non-smooth component of (5) and then performs

a quadratic approximation of the smooth component g every iteration:

$$x_{k+1} = \text{prox}_h(x_k - t_k \nabla g(x_k)),$$

where t_k denotes the step size at iteration k . [24] proposed a proximal gradient method for precision matrix estimation which possesses attractive theoretical properties as well as a linear convergence rate under a suitable step size. The authors define g, h as two continuous convex functions mapping the domain of covariance matrices (the positive definite cone \mathbb{S}_{++}^p) onto \mathbb{R} and jointly optimize them using Graphical ISTA [24]. G-ISTA conducts a backtracking line search for determining an optimal step size or specifies a constant step size of $\lambda_{\min}(\Theta_k)$ for problems with a small p . This algorithm uses the duality gap as a stopping criteria and achieves a linear rate of convergence in $O(\log \varepsilon)$ iterations to reach a tolerance of ε .

III. METHODOLOGY

A. Overview of OWL Estimators

We define the Graphical Order Weighted ℓ_1 (GOWL) estimator to be the solution to the following constrained optimization problem:

$$\min_{\Theta \succ 0} -\log \det \Theta + \text{tr}(\mathbf{S}\Theta) + \Omega_{\text{OWL}}(\Theta), \quad (7)$$

where

$$\Omega_{\text{OWL}}(\Theta) = \xi^T |\text{vechs}(\Theta)|_{\downarrow} = \sum_{i=1}^K \xi_i |\text{vechs}(\Theta)|_{[i]}. \quad (8)$$

Here $\Theta \in \mathbb{R}^{p \times p}$, $\text{vechs}(\Theta)_{[i]}$ is the i^{th} largest off-diagonal component in magnitude of Θ , $K = (p^2 - p)/2$, and $\xi_1 \geq \xi_2 \geq \dots \geq \xi_p \geq 0$. The proximal mapping of Ω_{OWL} denoted by $\text{prox}_{\Omega_{\text{OWL}}} : \mathbb{R}^{p \times p} \mapsto \mathbb{R}^{p \times p}$ can be efficiently computed with $O(n \log n)$ complexity using the *pool adjacent violators* (PAV) algorithm for isotonic regression outlined in [25].

In a similar way, we define the column-by-column Graphical Order Weighted ℓ_1 (ccGOWL) estimator to be the solution to the following unconstrained optimization problem:

$$\hat{\beta}_j = \arg \min_{\beta_j \in \mathbb{R}^{p-1}} \|\mathbf{X}_{*,j} - \mathbf{X}_{*,-j} \beta_j\|_2^2 + \Omega_{\text{OWL}}(\beta_j), \quad (9)$$

where $\beta_j \in \mathbb{R}^{p-1}$, with hyperparameters defined the same way as above. We then combine the β_j column vectors to form $\hat{\Theta}$. Figure 2 depicts the different ways that each estimator applies the OWL penalty. The GOWL estimator applies the penalty to the vectorized lower triangle of the precision matrix and the ccGOWL estimator applies the OWL penalty to the columns of the precision matrix separately.

B. Uniqueness of GOWL

In this section, we derive a dual formulation of GOWL. This formulation plays an important role for implementing efficient algorithms and allows us to establish uniqueness of the solution of GOWL. Introducing the dual variable $\mathbf{W} \in \mathbb{R}^{p \times p}$ and letting

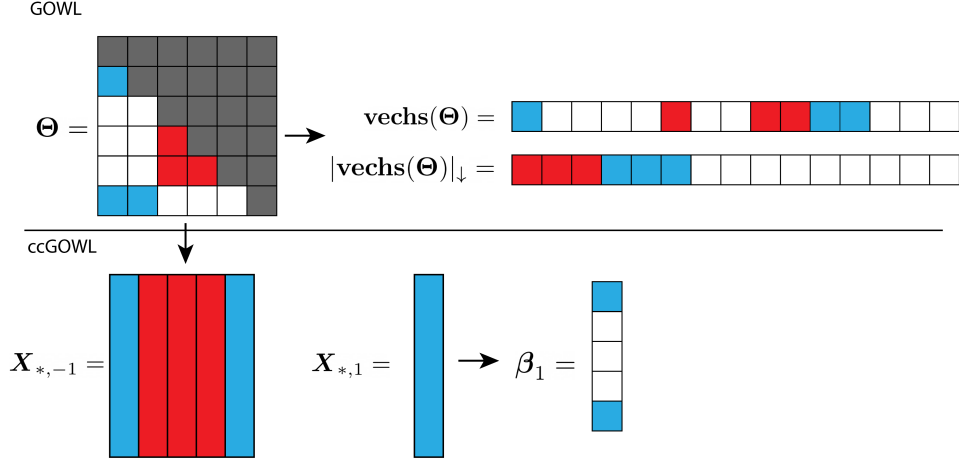


Fig. 2: The GOWL and ccGOWL frameworks—likelihood and column-by-column OWL penalized estimation procedures.

w_i denote the i -th entry of $\text{vech}(\mathbf{W})$, we can identify the dual problem as follows (see Appendix A for details).

$$\begin{aligned} \max_{\mathbf{W} \succ 0} \quad & \log \det (\mathbf{S} + \mathbf{W}) \\ \text{s.t.} \quad & |w_i| \leq \xi_i \quad \forall i, \\ & (\mathbf{S} + \mathbf{W}) \succ 0. \end{aligned} \quad (10)$$

The following proposition, which follows from the development in Appendix A, specifies the duality gap.

Proposition 1. *For the optimization problem (7) and the dual problem (10), the duality gap Δ given a point \mathbf{W} in the feasible set defined by $B_\lambda = \{\mathbf{W} : |\mathbf{W}_i| \leq \xi_i, \forall i, \mathbf{W} \in \mathbb{S}_{++}^p\}$ is*

$$\Delta = \text{tr}(\mathbf{S}\Theta) + \sum_{i=1}^K \xi_i |\Theta|_{[i]} - p. \quad (11)$$

where tr denotes the trace operator and \mathbf{W} denotes the dual variable in the Lagrangian formulation.

In practice, Δ is estimated using the difference between the primal and the dual and acts as a stopping criterion for the iterative procedure. As opposed to other sparse graph estimation techniques, our proposed objective function has a unique solution.

Theorem 1. *If $\xi_i > 0$ for all i , then problem (7) has a unique optimal point Θ^* .*

The proof is provided in Appendix B and involves selecting \mathbf{W} within $\text{interior}(B_\lambda) = \{\mathbf{W} : |\mathbf{W}_i| < \xi_i, \forall i, \mathbf{W} \in \mathbb{R}^p\}$ such that Slater's condition is satisfied.

C. Algorithms

Our work borrows from G-ISTA discussed in Section II-C for solving the non-smooth problem defined in (7); the details are outlined in Algorithm 1. In a similar way, Algorithm 2 is based on the proximal method for solving the OWL regularized linear regression proposed in [25] and has a convergence rate of $O(1/k)$. Algorithm 2 applies a proximal method p times and combines each column to arrive at the final precision matrix estimate. Code implementing these algorithms is available at <https://github.com/cmazzaanthony/ccgowl>.

Algorithm 1 Algorithm for GOWL

Require: \mathbf{S} , tolerance ε , ξ , $t_0 > 0$, Θ^0 , $c \in (0, 1)$

while $\Delta > \varepsilon$ **do**

(1) Let t_k be the largest element of $\{c^j t_{k,0}\}$ so that for $\Theta^{k+1} = \text{prox}_{\Omega_{\text{OWL}}}(\Theta^k - t_k(\mathbf{S} - ((\Theta^k)^{-1})))$, the following are satisfied:

$$\Theta^{k+1} \succ 0,$$

$$-\log \det \Theta^{k+1} + \text{tr}(\mathbf{S}\Theta^{k+1}) \leq Q_{t_k}(\Theta^{k+1}, \Theta^k),$$

where

$$\begin{aligned} Q_{t_k}(\Theta^{k+1}, \Theta^k) = & -\log \det \Theta + \text{tr}(\mathbf{S}\Theta) \\ & + \text{tr}((\Theta^{k+1} - \Theta^k)(\mathbf{S} - (\Theta^k)^{-1})) \\ & + \frac{1}{2t_k} \|\Theta^{k+1} - \Theta^k\|_F^2. \end{aligned}$$

(2) Set $\Theta_{t+1} := \text{prox}_{\text{OWL}}(\Theta^k - t_k(\mathbf{S} - (\Theta^k)^{-1}))$.

(3) Compute the duality gap Δ .

end while

Ensure: ε -optimal solution $\hat{\Theta}$.

D. Sufficient Grouping Conditions for ccGOWL

We can establish sufficient grouping conditions when estimating each column of Θ by drawing on previous work for the OSCAR and OWL regularizers [23]. The term “grouping” refers to components of each column estimate being equal.

Theorem 2. *Let $\hat{\beta}_k, \hat{\beta}_l > 0$ be elements in the column estimate $\hat{\beta}_j$ of Θ_j estimated by ccGOWL with hyperparameter λ_2 , and let $\mathbf{a}_k, \mathbf{a}_l$ be two columns of the matrix $\mathbf{X}_{*, -j}$ such that $\mathbf{1}^\top \mathbf{a}_k = 0, \mathbf{1}^\top \mathbf{a}_l = 0$ and $\|\mathbf{a}_k\|_2 = 1, \|\mathbf{a}_l\|_2 = 1$. Denote $\rho_{kl} = \mathbf{a}_k^\top \mathbf{a}_l \in [-1, 1]$. Then,*

$$\sqrt{2 - 2\rho_{kl}} < \lambda_2 / \|\mathbf{X}_{*, j}\|_2 \implies \hat{\beta}_k = \hat{\beta}_l. \quad (12)$$

Depending on the sample correlation between covariates in $\mathbf{X}_{*, -j} \in \mathbb{R}^{n \times (p-1)}$ and the value of λ_2 , the sufficient grouping property can be quantified according to Theorem 2. The proof is provided in Appendix C.

Algorithm 2 Algorithm for ccGOWL

Require: \mathbf{X} , tolerance ε , ξ , $t_0 > 0$
for $j \rightarrow p$ **do**

 (1) Determine $t_k > 0$ such that the following is satisfied:

$$\|\mathbf{X}_{*,j} - \mathbf{X}_{*,j}\beta_j^{k+1}\|_2^2 \leq Q_{t_k}(\beta_j^k, \beta_j^{k+1}),$$

where

$$\begin{aligned} Q_{t_k}(\beta_j^k, \beta_j^{k+1}) &= \|\mathbf{X}_{*,j} - \mathbf{X}_{*,j}\beta_j^{k+1}\|_2^2 \\ &\quad + 2(\beta_j^k - \beta_j^{k+1})^T \mathbf{X}_{*,j}^T (\beta_j^k - \beta_j^{k+1}) \\ &\quad + \frac{t_k}{2} \|\beta_j^k - \beta_j^{k+1}\|_2^2. \end{aligned}$$

(2) Compute

$$\nabla g(\beta_j^k) := \mathbf{X}_{*,j}^T (\mathbf{X}_{*,j} - \mathbf{X}_{*,j}\beta_j^k).$$

 (3) Set $\beta_j^{k+1} \leftarrow \text{prox}_{\text{OWL}}(\beta_j^k - t_k \nabla g(\beta_j^k))$.

 (4) Exit when $\|\beta_j^{k+1} - \beta_j^k\|_2 < \varepsilon$.

end for

 Combine all $\hat{\beta}_j^{k+1}$ to form $\hat{\Theta}$.

IV. EXPERIMENTAL RESULTS

To assess the performance of the proposed algorithms, we conducted a series of experiments: we first compared the estimates found by GOWL and ccGOWL to those from GRAB [4] and GLASSO [3] on a synthetic dataset with controlled sparsity and grouping. Then, we compared the average weighted F_1 scores [26] obtained by all four algorithms on random positive definite grouped matrices of varying size and group density. Additional results for the synthetic data, including absolute error and mean squared error metrics for prediction of precision matrix entries, are reported in Appendix E. Hyperparameters λ_1 and λ_2 using the OSCAR weight generation defined in Section 3.3 were selected using a 2-fold standard cross-validation procedure. Similar to [4], the regularization parameter for the GRAB estimator was also selected using a 2-fold cross-validation procedure (see Appendix D for details). All algorithms were implemented in Python and executed on an Intel i7-8700k 3.20 GHz and 32 GB of RAM.

A. Synthetic Data

Synthetic data was generated by first creating a proportion of groups $\kappa \in \{0.1, 0.2\}$ for a p -dimensional matrix. We randomly chose each group size to be between a minimum size of 0.1 of p and a maximum size of 0.4 of p . Furthermore, group values were determined by uniformly sampling their mean between $(0.9, 1.0)$ and $(-0.9, -1.0)$ respectively. After setting all values of a given group to its mean, we collect the groups into the matrix Θ^* . In order to add noise to the true group values, we randomly generated a positive semi-definite matrix with entries set to zero with a fixed probability of 0.5 and remaining values sampled between $(-0.1, 0.1)$. We then added the grouped matrix to the aforementioned noise matrix to create a $\Theta^* + \epsilon$ matrix. Each grouped matrix was generated 5 times

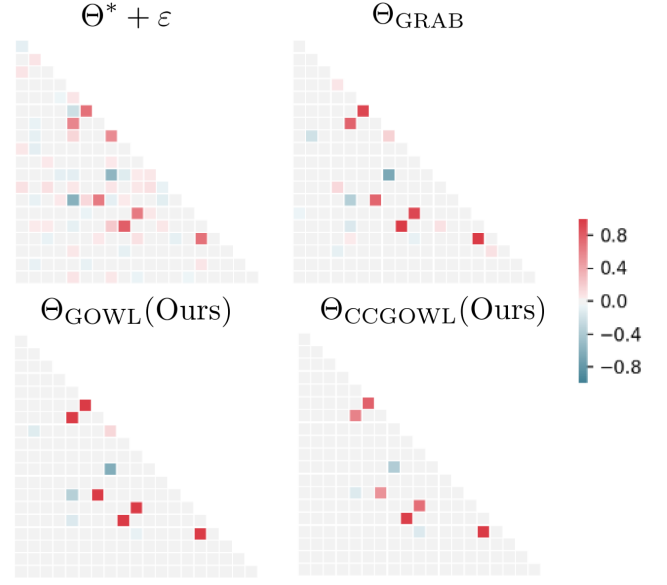


Fig. 3: Synthetic data results example for methods ccGOWL/GOWL precision matrices with $p = 20$ and $\kappa = 0.1$.

and random noise matrices were added to each of the 5 grouped matrices 20 times. A dataset was then generated by drawing i.i.d. from a $\mathcal{N}_p(0, (\Theta^* + \epsilon)^{-1})$ distribution. The empirical covariance matrix can be estimated after standardization of covariates.

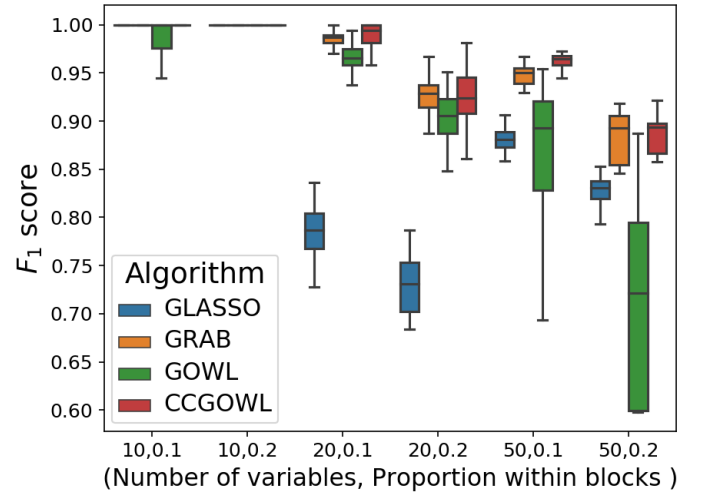


Fig. 4: Quantiles of weighted F_1 score metric for GLASSO, GRAB, GOWL, CCGOWL.

Figure 3 shows an example of a synthetic precision matrix with 2 groups with Θ^* as the ground truth. This ground truth was then used to sample a dataset of $n = 100$, from which we estimated the empirical covariance matrix and provided it as input to the algorithms. The GOWL and ccGOWL precision matrix estimates almost fully recover the 6 red entries from group 1 and the two blue entries from group two. The GLASSO was not included as a result of its poor

performance in recovering the true group values. We assessed the performance of all three methods using the weighted F_1 classification score (harmonic mean of precision and recall) since we are interested in multi-group classification. The F_1 score is defined as $F_1 = 2 \cdot \frac{\text{precision} \cdot \text{recall}}{\text{precision} + \text{recall}}$; the weighted F_1 score is obtained by calculating the F_1 score for each label and then evaluating the weighted average, where the weights are proportional to the number of true instances of each group. For each value of $(p, \kappa) \in \{10, 20, 50\} \times \{0.1, 0.2\}$, we generated 5 randomly grouped matrices using the procedure outlined in the previous section and fit GLASSO, GRAB, GOWL, ccGOWL to each of them. The estimates were then clustered using a Gaussian Mixture Model (GMM) with the same number of groups as originally set. The identification of the clusters was compared to the original group labeling using the weighted F_1 metric, from which we report the permutation of labels giving the highest weighted F_1 score. Figure 4 shows the distribution of the scores for each algorithm, for each class of matrices. Overall, the ccGOWL outperforms GOWL and GLASSO in terms of variance and mean of F_1 scores. The reason the ccGOWL outperforms GOWL could be due to the fact that with GOWL we have to generate many more parameters since we penalize the entire set of edges together as opposed to one column at a time. We observe that ccGOWL achieves similar or better performance when compared to GRAB. Mean squared error and absolute error were also measured for each estimate and are provided in Appendix E.

TABLE I: Timing Comparisons in Seconds

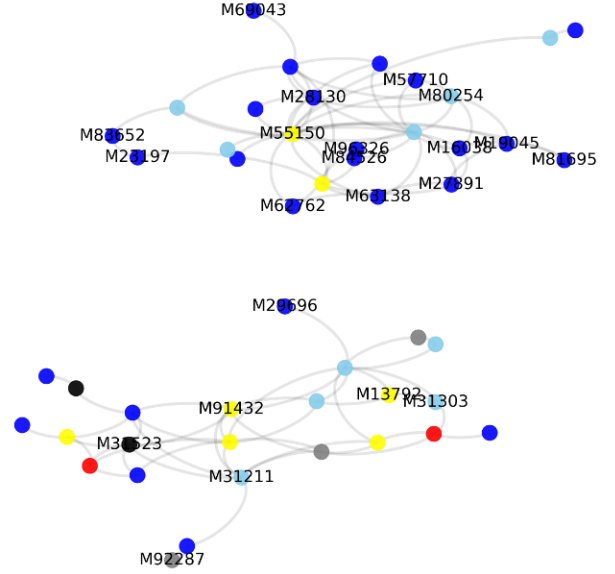
Method	$p = 10$	$p = 20$	$p = 50$	$p = 100$	$p = 500$	$p = 1000$
GLASSO	0.006	0.012	0.017	0.023	0.118	0.456
GRAB	0.071	0.096	0.466	1.243	51.225	499.225
ccGOWL	0.003	0.012	0.034	0.095	0.305	4.126

B. Timing Comparisons

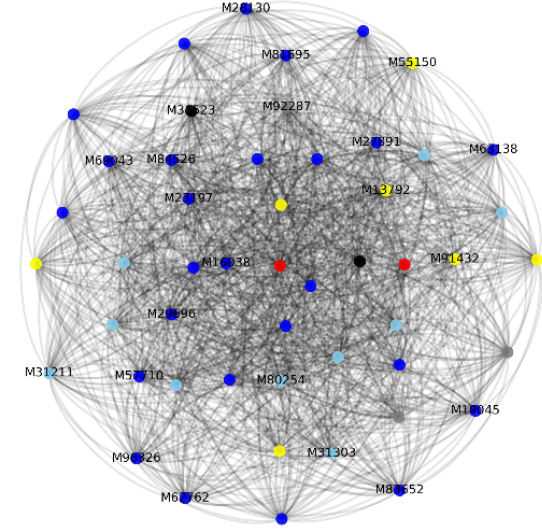
The GLASSO, GRAB and ccGOWL algorithms were run on synthetic datasets generated in the same way as in Section IV-A with varying p , $n = 100$, $\kappa = 0.2$ and different levels of regularization. The GRAB algorithm had a fixed duality gap of 10^{-4} and the ccGOWL had a fixed precision of 10^{-5} . The GRAB algorithm was implemented in `python` and uses the R package `QUIC`, implemented in C++ [27], to find the optimum of the log-likelihood function. The ccGOWL algorithm is implemented completely in `python` and requires solving p linear regressions with most of the computational complexity attributed to evaluating the proximal mapping. The GLASSO algorithm uses the `python` package `sklearn` [28]. Running times are presented in Table I and show a significant advantage of ccGOWL over GRAB. This difference for large p is due to GRAB requiring matrix inversions within `QUIC` ($O(p^2)$) and applying the k-means clustering algorithm ($O(pK)$) on the rows of the block matrix Z .

C. Cancer Gene Expression Data

We consider a dataset that uses expression monitoring of genes using DNA microarrays in 38 patients that have been



(a) Network constructed by ccGOWL on gene expression data ($\lambda_1 = 0.3$, $\lambda_2 = 0.00612821$).



(b) Network constructed by GLASSO on gene expression data with $\lambda = 0.4$.

Fig. 5: The ccGOWL network estimate clearly groups genes associated with AML (top) and ALL (bottom). Each color represents a biological pathway: Signal Transduction (red), Immune System (blue), Cell Cycle (gray), Metabolism (yellow), Gene Expression (black), Uncategorized (skyblue).

diagnosed with either acute myeloid leukemia (AML) or acute lymphoblastic leukemia (ALL). This dataset was initially investigated in [29]. In order to allow for a model that is easier to interpret we selected the 50 most highly correlated genes associated with ALL-AML diseases, as identified in [29]. Expression levels were standardized to have zero mean and unit variance. Of the 50 genes selected, the first 25 genes are known to be highly expressed in ALL and the remaining 25 genes are known to be highly expressed in AML. It is important to note that no single gene is consistently expressed

across both AML and ALL patients. This fact illustrates the need for an estimation method that takes into account multiple genes when diagnosing patients. Edges between genes that are highly expressed in AML should appear in the same group and likewise for the ALL disease. In addition, we use the Reactome database [30] to identify each gene's main biological pathway.

Figure 5a illustrates that ccGOWL groups genes according to their disease. In fact, ccGOWL correctly identifies all 25 genes associated with the AML disease in one group and 24 of 25 genes associated with the ALL disease in the other group (Appendix F, Table VII). We compare the network identified by ccGOWL with the commonly-used baseline GLASSO method, to illustrate the importance of employing an estimator that uses grouping (Figure 5b). In addition, examining the connections within each group can also lead to useful insights. The AML group (top) contains highly connected genes beginning with “M” (blue nodes) which are associated with the neutrophil granulation process in the cell. AML is a disorder in the production of neutrophils [31]. Neutrophils are normal white blood cells with granules inside the cell that fight infections. AML leads to the production of immature neutrophils (referred to as blasts), leading to large infections.

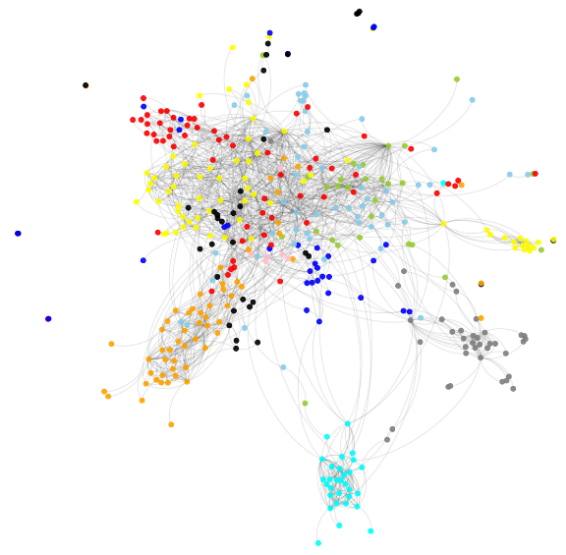
D. Equities Data

We consider the stock price dataset described in [32], which is available in the huge package on CRAN [33]. The dataset consists of the closing prices of stocks in the S&P 500 between January 1, 2003 and January 1, 2008. The collection of stocks can be categorized into 10 Global Industry Classification Standard (GICS) sectors [34]. Stocks that were not consistently in the S&P 500 index or were missing too many closing prices were removed from the dataset.

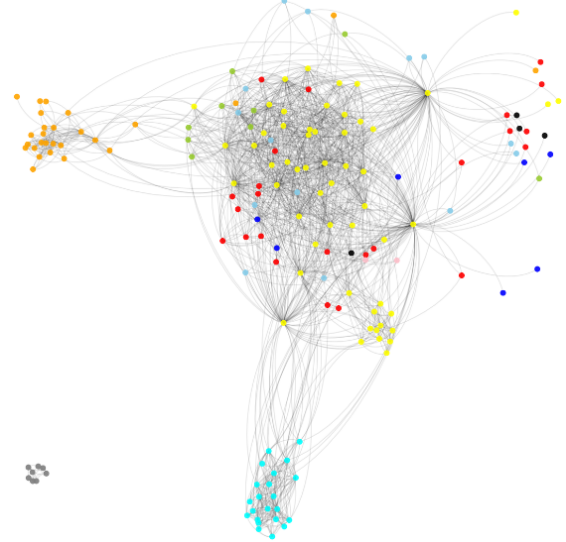
The design matrix $\mathbf{X} \in \mathbb{R}^{1257 \times 452}$ contains the log-ratio of the price at time t to the price at time $t - 1$ for each of the 452 stocks for 1257 trading days. More formally we write that the (i, j) -th entry of \mathbf{X} is defined as $x_{ij} = \log(S_{(i+1)j}/S_{ij})$ where S_{ij} is the closing price of the j th stock on the i th day. The matrix \mathbf{X} is then standardized so each stock has a mean of zero and unit variance. The GICS sector for each stock is known, but this information was not used when estimating the precision matrix based on the returns matrix \mathbf{X} . Figure 6a illustrates the ability of ccGOWL to group relationships between stocks that belong to the same sector. The identified network is more interpretable than the network constructed by GLASSO (Figure 6b). Information Technology and Utilities largely exhibit conditional independence of stocks in other GICS sectors. On the other hand, there appears to be a conditional dependence between stocks in the Materials and Industrials sectors, probably as a result of multiple customer-supplier relationships between the companies in these sectors. Both sectors are sensitive to economic cycles and the equities offer exposure to global infrastructure replacement.

V. CONCLUSION AND FUTURE WORK

We proposed the GOWL and ccGOWL estimators—two novel precision matrix estimation procedures based on the Order Weighted ℓ_1 norm. We proved the uniqueness of the



(a) Network constructed by ccGOWL on equities expression data ($\lambda_1 = 0.4$, $\lambda_2 = 0.0001$).



(b) Network constructed by GLASSO on equities expression data with $\lambda = 0.1$.

Fig. 6: Each colour represents a GICS sector: Consumer Discretionary (red), Consumer Staples (blue), Energy (gray), Financials (yellow), Health Care (black), Industrials (skyblue), Information Technology (orange), Materials (yellow-green), Telecommunications Services (pink), Utilities (cyan).

GOWL estimator and identified sufficient grouping conditions for the ccGOWL estimator. Based on empirical results on synthetic and real datasets, the ccGOWL estimator has the ability to accurately identify structure in the precision matrix in a much more computationally efficient manner than state-of-the-art estimators that achieve comparable accuracy. It is also important to mention that we believe a norm consistency result would be desirable and it could be an interesting topic of future work. This result could be achieved by following the strategy proposed in [35] which imposes assumptions on the design matrix and deviation bound between predictors

and the error term. Although penalized likelihood methods for learning structure in precision matrix estimation are widely used and perform well, it is also important to consider column-by-column estimators that accomplish similar feats while reducing computational complexity.

APPENDIX A

DUAL PROBLEM FORMULATION FOR GOWL

The following formulation uses the technique from [7]. Let $\mathbf{Z} = \mathbf{\Theta}$ and its associated dual variable be $\mathbf{W} \in \mathbb{R}^{p \times p}$, which gives the Lagrangian:

$$\mathcal{L}(\mathbf{\Theta}, \mathbf{Z}, \mathbf{W}) = -\log \det \mathbf{\Theta} + \text{tr}(\mathbf{S}\mathbf{\Theta}) + \sum_{i=1}^K \xi_i |\text{vechs}(\mathbf{Z})|_{[i]} + \text{tr}(\mathbf{W}(\mathbf{\Theta} - \mathbf{Z})), \quad (13)$$

Note that the above quantity is separable into terms involving $\mathbf{\Theta}$ and \mathbf{Z} , thus allowing computation of the infimum over the auxiliary variables. We first consider the terms involving \mathbf{Z} or more precisely, its vectorized form $\mathbf{z} = \text{vechs}(\mathbf{Z})$:

$$g(\mathbf{z}) = \xi_{\downarrow}^T \mathbf{z}_{\downarrow} - \text{tr}(\mathbf{W}\mathbf{Z}).$$

By the generalized rearrangement inequality [36], we know that for arbitrary vectors ξ, \mathbf{w} , $\xi_{\downarrow}^T \mathbf{w}_{\uparrow} \leq \xi^T \mathbf{w} \leq \xi_{\uparrow}^T \mathbf{w}_{\downarrow}$ and hence if $\xi_i \geq |\mathbf{w}_i|$ for $i = 1, \dots, K$ and $\mathbf{w} = \text{vechs}(\mathbf{W})$, then $\inf_{\mathbf{z}} g(\mathbf{z}) = 0$. Otherwise, the problem is unbounded and the infimum is attained at $g(\mathbf{z}) = -\infty$. Therefore

$$\inf_{\mathbf{z}} \sum_{i=1}^K \xi_i |\mathbf{z}_{[i]}| - \text{tr}(\mathbf{W}\mathbf{Z}) = \begin{cases} 0 & \text{if } \xi_i \geq |\mathbf{w}_i| \\ & \text{for } i = 1, \dots, K, \\ -\infty & \text{otherwise.} \end{cases} \quad (14)$$

The infimum over terms involving $\mathbf{\Theta}$ can be computed by taking the gradient of the log determinant under the assumption that $\mathbf{S} + \mathbf{W} \succ 0$ and is attained at the point:

$$\inf_{\mathbf{\Theta}} [-\log \det \mathbf{\Theta} + \text{tr}((\mathbf{S} + \mathbf{W})\mathbf{\Theta})] = \log \det(\mathbf{S} + \mathbf{W}) + p. \quad (15)$$

Combining (13) with the constraint (14) and letting w_i denote the i -th entry of $\text{vechs}(\mathbf{W})$ allows us to write the dual as:

$$\begin{aligned} \max_{\mathbf{W} \succ 0} \quad & \log \det(\mathbf{S} + \mathbf{W}) \\ \text{s.t.} \quad & |w_i| \leq \xi_i \quad \forall i, \\ & (\mathbf{S} + \mathbf{W}) \succ 0. \end{aligned} \quad (16)$$

If we define the feasible set $B_{\lambda} = \{\mathbf{W} : |\mathbf{W}_i| \leq \xi_i, \forall i, \mathbf{W} \in \mathbb{S}_{++}^p\}$, then for any feasible dual point $\mathbf{W} \in B_{\lambda}$ the corresponding primal point $\mathbf{\Theta} = (\mathbf{S} + \mathbf{W})^{-1}$. From (14), (15) and (7), we see that the duality gap Δ is defined by:

$$\begin{aligned} \Delta &= \left(-\log \det(\mathbf{S} + \mathbf{W}) + \text{tr}(\mathbf{S}\mathbf{\Theta}) + \sum_{i=1}^K \xi_i |\mathbf{\Theta}|_{[i]} \right) \\ &\quad - (\log \det(\mathbf{S} + \mathbf{W}) + p), \\ &= \text{tr}(\mathbf{S}\mathbf{\Theta}) + \sum_{i=1}^K \xi_i |\mathbf{\Theta}|_{[i]} - p \end{aligned} \quad (17)$$

APPENDIX B PROOF OF THEOREM 1

The following proof uses the technique from [7] and builds upon Slater's condition as formulated in the following theorem:

Slater's condition. *Let a constrained optimization problem be of the form:*

$$\begin{aligned} \min_{\mathbf{x} \in \mathcal{X}} \quad & f(\mathbf{x}) \\ \text{s.t.} \quad & g_i(\mathbf{x}) \leq 0 \quad (i = 1, \dots, m), \\ & h_j(\mathbf{x}) = 0 \quad (j = 1, \dots, p), \end{aligned} \quad (18)$$

We say that the Slater constraint qualification (SCQ) holds for (18) if there exists $\hat{\mathbf{x}} \in \mathcal{X}$ such that

$$g_i(\hat{\mathbf{x}}) < 0 \quad \text{and} \quad h_j(\hat{\mathbf{x}}) = 0.$$

Furthermore, if $\hat{\mathbf{x}} \in \text{interior}(\mathcal{X})$, then strong duality holds at the point $\hat{\mathbf{x}}$.

First, assume that $c = \max_{i,j} |\mathbf{S}|_{ij}$ is known. In the case where \mathbf{S} is standardized, $c = 1$. The negative log-likelihood is convex in the precision matrix and is defined over the set of all positive-definite matrices. On the other hand, the OWL estimator is also convex in $\mathbf{\Theta}$ over the same set. Since the sum of two convex functions over the same convex set is convex, we conclude that the main objective is convex.

Using the SCQ, we can say that the duality gap is zero and write the primal-dual optimal pair in the following way:

$$\mathbf{\Theta}^* = (\mathbf{S} + \mathbf{W}^*)^{-1}.$$

For the SCQ to hold, it remains to show that there exists a point \mathbf{W} in the interior of the feasible set given by $\text{interior}(B_{\lambda}) = \{\mathbf{W} : |\mathbf{W}_i| < \xi_i, \forall i, \mathbf{W} \in \mathbb{R}^p\}$ such that it is the solution of (14).

The goal is to choose a \mathbf{W} such that $(\mathbf{S} + \mathbf{W}) \succ 0$ and ensure that the entries $|\mathbf{W}_i|$ are close to zero. First recall that \mathbf{S} is a symmetric positive semi-definite matrix and since it was estimated from data, we can assume that the diagonal entries will be greater than zero with probability one. Let $\mathbf{A} = \text{diag}(\mathbf{S}) \succ 0$ since the determinant of a diagonal matrix with positive entries is positive. Consequently, by Sylvester's criterion, \mathbf{A} is positive definite (PD). We can then write the convex combination of \mathbf{S} and \mathbf{A} as

$$\alpha \mathbf{S} + (1 - \alpha) \mathbf{A} \succ 0.$$

where $\alpha \in [0, 1)$. The above expression is itself positive definite, which we can see by taking any $\mathbf{x} \in \mathbb{R}^p$:

$$\begin{aligned} \mathbf{x}^T (\alpha \mathbf{S} + (1 - \alpha) \mathbf{A}) \mathbf{x} &= \mathbf{x}^T (\alpha \mathbf{S}) \mathbf{x} + \mathbf{x}^T ((1 - \alpha) \mathbf{A}) \mathbf{x} \\ &= \alpha \underbrace{(\mathbf{x}^T \mathbf{S} \mathbf{x})}_{\geq 0} + (1 - \alpha) \underbrace{(\mathbf{x}^T \mathbf{A} \mathbf{x})}_{\geq 0} > 0 \\ &> 0. \end{aligned}$$

Thus, we can write

$$\mathbf{S} + \mathbf{W} = \alpha \mathbf{S} + (1 - \alpha) \mathbf{A} \succ 0,$$

for non-negative α strictly smaller than 1. For a given matrix of hyperparameters \mathbf{A} , pick $\alpha > 1 - 1/c \min_{kl} \mathbf{A}_{kl}$. In practice

this can be achieved by setting $\tilde{\alpha} = 1 - 1/c \min_{kl} \mathbf{A}_{kl}$ and putting $\alpha = \tilde{\alpha} + \varepsilon$ for some $\varepsilon > 0$. Then,

$$\begin{aligned} \mathbf{W} &= \alpha \mathbf{S} + (1 - \alpha) \mathbf{A} - \mathbf{S} \\ &= (1 - \alpha)(\mathbf{A} - \mathbf{S}), \end{aligned}$$

and hence

$$\begin{aligned} |\mathbf{W}|_{ij} &= (1 - \alpha) |\mathbf{S}|_{ij} \quad (i, j = 1, \dots, p) \\ &< 1/c \min_k \xi_k |\mathbf{S}|_{ij} \\ &\leq \min_k \xi_k \\ &\leq \xi_{ij}. \end{aligned}$$

Here we used the fact that the values in the empirical estimate of the covariance matrix \mathbf{S} cannot be infinite. By the convexity of the primal objective and SCQ, we conclude that \mathbf{W}^* is unique. Furthermore, since the duality gap is zero at the point \mathbf{W}^* , the uniqueness of \mathbf{W}^* implies the uniqueness of Θ^* . ■

APPENDIX C PROOF OF THEOREM 2

The following proof uses the technique from [23]. First, we define the smallest gap of consecutive elements of ξ as $\lambda_2 = \min_l \{\xi_l - \xi_{l-1} : 1 \leq l \leq p-1\}$. Consider a pair of column estimates $\hat{\beta}_k$ and $\hat{\beta}_l$ with associated columns of the matrix $\mathbf{X}_{*,j}$ denoted a_k, a_l respectively, for which $\|\mathbf{X}_{*,j}\|_2 \|a_k - a_l\| < \Delta_\lambda$.

Let $L_2(\beta_j) = \|\mathbf{X}_{*,j}\beta_j - \mathbf{X}_{*,j}\|_2^2$ and let $f(\beta_j) = L_2(\beta_j) + \Omega_\lambda(\beta_j)$. Consider the directional derivative of f at a point $\hat{\beta}_j$ in direction \mathbf{u} . Following the argument of [23], we see that

$$f'(\hat{\beta}_j, \mathbf{u}) \leq \|\mathbf{X}_{*,j}\|_2 \|a_k - a_l\| - \lambda_2, \quad (19)$$

which implies that $\hat{\beta}_j$ is not a minimizer of $f(\cdot, \mathbf{u})$. It follows from the contradiction argument that $\hat{\beta}_k = \hat{\beta}_l$ if $\|\mathbf{X}_{*,j}\|_2 \|a_k - a_l\| < \lambda_2$ holds. ■

APPENDIX D HYPER-PARAMETER SPECIFICATION

Tables II, III, and IV list the hyper-parameters chosen for the synthetic data in Section IV-A. The hyper-parameters were chosen using a 2-fold cross-validation procedure. For the gene dataset in Section IV-C the hyperparameters used were $\lambda_1 = 0.3$ and $\lambda_2 = 0.00612821$ and were chosen by using the λ_1, λ_2 provided by 2-fold cross-validation and then the sparsity hyperparameter was increased to encourage more sparsity. For the stock dataset in Section IV-D the hyperparameters used were $\lambda_1 = 0.2$ and $\lambda_2 = 0.0001$. The hyperparameters were chosen arbitrarily as cross-validation required too much computational resources.

APPENDIX E

SYNTHETIC DATA: ADDITIONAL EXPERIMENTAL RESULTS

Figures 7 and 8 show the absolute error and mean squared error for estimation of the precision matrix entries for the synthetic data experiments in Section IV-A. The ccGOWL

TABLE II: GOWL Hyper-parameter Specification

p	Block %	λ_1	λ_2	Range Considered
10	10	0.03684211	0.01052632	(0, 0.1)
10	20	0.06842105	0.01052632	(0, 0.1)
20	10	0.06551724	0.00344828	(0, 0.1)
20	20	0.02413793	0.00344828	(0, 0.1)
50	10	0.008	0.00010	(0, 0.1)
50	20	0.006	0.00009	(0, 0.1)

TABLE III: ccGOWL Hyper-parameter Specification

p	Block %	λ_1	λ_2	Range Considered
10	10	0.10526316	0.05263158	(0, 0.1)
10	20	0.10526316	0.05263158	(0, 0.1)
20	10	0.23684211	0.00793103	(0, 0.1)
20	20	0.23684211	0.00793103	(0, 0.1)
50	10	0.1	0.00512821	(0, 0.1)
50	20	0.1	0.00512821	(0, 0.1)

TABLE IV: GRAB Hyper-parameter Specification

p	Block %	λ	Range Considered
10	10	0.1	(0, 1.0)
10	20	0.1	(0, 1.0)
20	10	0.7	(0, 1.0)
20	20	0.5	(0, 1.0)
50	10	0.5	(0, 1.0)
50	20	0.4	(0, 1.0)

estimator has a lower mean squared error and absolute error for $p = 20$ and $p = 50$ and has slightly higher errors for $p = 10$. For larger values of p , the performance discrepancy between ccGOWL and GRAB is more noticeable for these metrics than for the weighted F_1 scores.

Table V and VI provide additional results, comparing the F_1 , MSE, sensitivity and specificity of the three methods while varying parameters p , κ , and n . These Tables illustrate that the ccGOWL method has lower mean square error in most cases even for a wider range of parameters. Likewise, the specificity and sensitivity values are also larger in most cases.

p	κ	n	GRAB		GOWL		CCGOWL	
			F_1	MSE	F_1	MSE	F_1	MSE
15	0.1	1000	1.00	2.01	1.00	5.96	1.00	2.43
15	0.1	2000	1.00	1.90	1.00	6.99	1.00	1.57
15	0.3	1000	0.42	3.06	0.48	6.65	0.61	1.51
15	0.3	2000	0.50	2.39	0.39	7.42	0.60	1.62
25	0.1	1000	0.71	4.55	0.89	8.13	0.87	0.80
25	0.1	2000	0.73	4.99	0.69	6.23	0.71	1.78
25	0.3	1000	0.30	1.04	0.14	6.20	0.26	1.23
25	0.3	2000	0.23	1.05	0.20	6.25	0.30	3.10

TABLE V: Additional Simulations: F_1 and MSE scores over 10 replications.

APPENDIX F GENE EXPRESSION DATA

Table VII shows which genes are highly expressed in individuals with either the ALL or AML disease as demonstrated in [29].

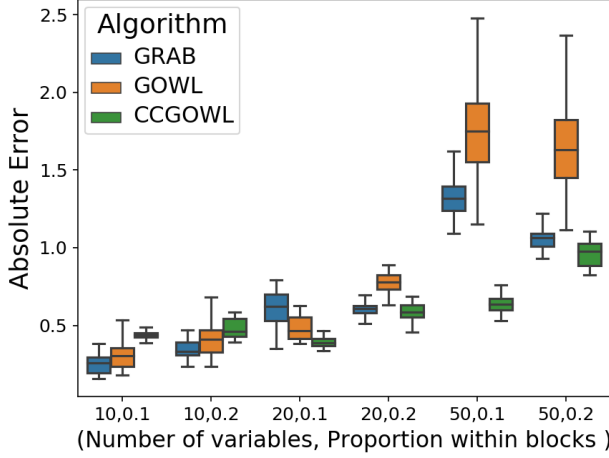


Fig. 7: Absolute Error Values for GRAB, GOWL, and ccGOWL for the synthetic data in Section IV-A.

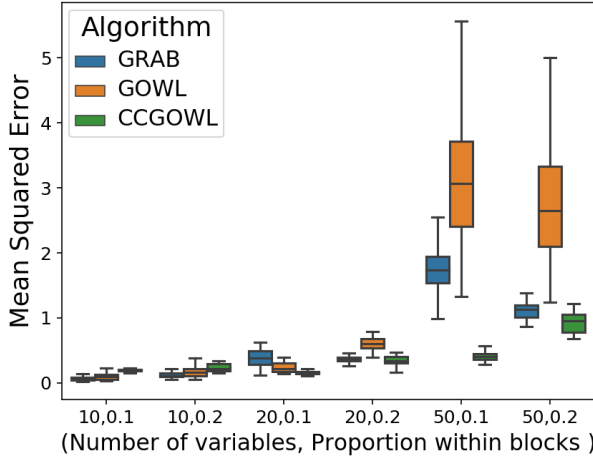


Fig. 8: Mean Squared Error Values for GRAB, GOWL, and ccGOWL for the synthetic data in Section IV-A.

p	κ	n	GRAB		GOWL		CCGOWL	
			Sens.	Spec.	Sens.	Spec.	Sens.	Spec.
15	0.1	1000	1.00	1.00	1.00	1.00	1.00	1.00
15	0.1	2000	1.00	1.00	1.00	1.00	1.00	1.00
15	0.3	1000	0.30	0.34	0.20	0.47	0.33	0.90
15	0.3	2000	0.30	0.47	0.10	0.38	0.55	0.66
25	0.1	1000	0.59	0.98	1.00	0.97	0.86	0.99
25	0.1	2000	0.73	0.97	0.60	0.97	0.50	0.99
25	0.3	1000	0.00	0.33	0.00	0.20	0.30	0.20
25	0.3	2000	0.20	0.30	0.10	0.52	0.30	0.35

TABLE VI: Additional Simulations: Sensitivity and specificity scores over 10 replications.

REFERENCES

[1] W. E. Peterman, B. H. Ousterhout, T. L. Anderson, D. L. Drake, R. D. Semlitsch, and L. S. Eggert, "Assessing modularity in genetic networks to manage spatially structured metapopulations," *Ecosphere*, vol. 7, no. 2, 2016.

[2] E. A. Stone and J. F. Ayroles, "Modulated modularity clustering as an exploratory tool for functional genomic inference," *PLoS Genetics*, vol. 5, no. 5, p. e1000479, 2009.

TABLE VII: Gene Classification

ALL	AML
U22376	M55150
X59417	X95735
U05259	U50136
M92287	M16038
M31211	U82759
X74262	M23197
D26156	M84526
S50223	Y12670
M31523	M27891
L47738	X17042
U32944	Y00787
Z15115	M96326
X15949	U46751
X63469	M80254
M91432	L08246
U29175	M62762
Z69881	M28130
U20998	M63138
D38073	M57710
U26266	M69043
M31303	M81695
Y08612	X85116
U35451	M19045
M29696	M83652
M13792	X04085

[3] J. Friedman, T. Hastie, and R. Tibshirani, "Sparse inverse covariance estimation with the graphical lasso," *Biostatistics*, vol. 9, no. 3, pp. 432–441, 2008.

[4] M. J. Hosseini and S.-I. Lee, "Learning sparse Gaussian graphical models with overlapping blocks," in *Advances in Neural Information Processing Systems*, 2016, pp. 3808–3816.

[5] K. M. Tan, D. Witten, and A. Shojaie, "The cluster graphical lasso for improved estimation of Gaussian graphical models," *Computational Statistics & Data Analysis*, vol. 85, pp. 23–36, 2015.

[6] A. Defazio and T. S. Caetano, "A convex formulation for learning scale-free networks via submodular relaxation," in *Advances in Neural Information Processing Systems*, 2012, pp. 1250–1258.

[7] J. Duchi, S. Gould, and D. Koller, "Projected subgradient methods for learning sparse Gaussians," in *Proc. Int. Conf. Artificial Intelligence and Statistics*, 2008, pp. 153–160.

[8] T. Cai, W. Liu, and X. Luo, "A constrained ℓ_1 minimization approach to sparse precision matrix estimation," *Journal of the American Statistical Association*, vol. 106, no. 494, pp. 594–607, 2011.

[9] N. Meinshausen, P. Bühlmann *et al.*, "High-dimensional graphs and variable selection with the lasso," *The Annals of Statistics*, vol. 34, no. 3, pp. 1436–1462, 2006.

[10] S. Sun, H. Wang, and J. Xu, "Inferring block structure of graphical models in exponential families," in *Proc. Int. Conf. Artificial Intelligence and Statistics*, 2015, pp. 939–947.

[11] W. Lee and Y. Liu, "Joint estimation of multiple precision matrices with common structures," *The Journal of Machine Learning Research*, vol. 16, no. 1, pp. 1035–1062, 2015.

[12] J. Wang, "Joint estimation of sparse multivariate regression and conditional graphical models," *Statistica Sinica*, pp. 831–851, 2015.

[13] T. T. Cai, H. Li, W. Liu, and J. Xie, "Joint estimation of multiple high-dimensional precision matrices," *Statistica Sinica*, vol. 26, no. 2, p. 445, 2016.

[14] E. Devijver and M. Gallopin, "Block-diagonal covariance selection for high-dimensional Gaussian graphical models," *Journal of the American Statistical Association*, vol. 113, no. 521, pp. 306–314, 2018.

[15] S. Kumar, J. Ying, J. V. d. M. Cardoso, and D. Palomar, "A unified framework for structured graph learning via spectral constraints," *arXiv preprint arXiv:1904.09792*, 2019.

[16] D. A. Tarzanagh and G. Michailidis, "Estimation of graphical models through structured norm minimization," *Journal of Machine Learning Research*, vol. 18, no. 1, 2018.

[17] H. D. Bondell and B. J. Reich, "Simultaneous regression shrinkage, variable selection, and supervised clustering of predictors with OSCAR," *Biometrics*, vol. 64, no. 1, pp. 115–123, 2008.

- [18] D. Koller, N. Friedman, and F. Bach, *Probabilistic graphical models: principles and techniques*. MIT Press, 2009.
- [19] M. Wytock and Z. Kolter, "Sparse Gaussian conditional random fields: Algorithms, theory, and application to energy forecasting," in *Proc. Int. Conf. Machine Learning*, 2013, pp. 1265–1273.
- [20] H. Zou and T. Hastie, "Regularization and variable selection via the elastic net," *Journal of the Royal Statistical Society: Series B*, vol. 67, no. 2, pp. 301–320, 2005.
- [21] R. Tibshirani, M. Saunders, S. Rosset, J. Zhu, and K. Knight, "Sparsity and smoothness via the fused lasso," *Journal of the Royal Statistical Society: Series B*, vol. 67, no. 1, pp. 91–108, 2005.
- [22] M. Bogdan, E. Van Den Berg, C. Sabatti, W. Su, and E. J. Candès, "SLOPE—adaptive variable selection via convex optimization," *The Annals of Applied Statistics*, vol. 9, no. 3, p. 1103, 2015.
- [23] M. Figueiredo and R. Nowak, "Ordered weighted ℓ_1 regularized regression with strongly correlated covariates: Theoretical aspects," in *Proc. Int. Conf. Artificial Intelligence and Statistics*, 2016, pp. 930–938.
- [24] B. Rolfs, B. Rajaratnam, D. Guillot, I. Wong, and A. Maleki, "Iterative thresholding algorithm for sparse inverse covariance estimation," in *Advances in Neural Information Processing Systems*, 2012, pp. 1574–1582.
- [25] X. Zeng and M. A. Figueiredo, "The ordered weighted ℓ_1 norm: Atomic formulation, projections, and algorithms," *arXiv preprint arXiv:1409.4271*, 2014.
- [26] C. Manning, P. Raghavan, and H. Schütze, "Introduction to information retrieval," *Natural Language Engineering*, vol. 16, no. 1, pp. 100–103, 2010.
- [27] C.-J. Hsieh, M. A. Sustik, I. S. Dhillon, and P. K. Ravikumar, "Sparse inverse covariance matrix estimation using quadratic approximation," in *Advances in Neural Information Processing Systems*, 2011, pp. 2330–2338.
- [28] F. Pedregosa, G. Varoquaux, A. Gramfort, V. Michel, B. Thirion, O. Grisel, M. Blondel, P. Prettenhofer, R. Weiss, V. Dubourg, J. Vanderplas, A. Passos, D. Cournapeau, M. Brucher, M. Perrot, and E. Duchesnay, "Scikit-learn: Machine learning in Python," *Journal of Machine Learning Research*, vol. 12, pp. 2825–2830, 2011.
- [29] T. R. Golub, D. K. Slonim, P. Tamayo, C. Huard, M. Gaasenbeek, J. P. Mesirov, H. Coller, M. L. Loh, J. R. Downing, M. A. Caligiuri *et al.*, "Molecular classification of cancer: class discovery and class prediction by gene expression monitoring," *Science*, vol. 286, no. 5439, pp. 531–537, 1999.
- [30] D. Croft, A. F. Mundo, R. Haw, M. Milacic, J. Weiser, G. Wu, M. Caudy, P. Garapati, M. Gillespie, M. R. Kamdar *et al.*, "The reactome pathway knowledgebase," *Nucleic Acids Research*, vol. 42, no. D1, pp. D472–D477, 2013.
- [31] F. R. Davey, W. N. Erber, K. C. Gatter, and D. Y. Mason, "Abnormal neutrophils in acute myeloid leukemia and myelodysplastic syndrome," *Human Pathology*, vol. 19, no. 4, pp. 454–459, 1988.
- [32] H. Liu, F. Han, M. Yuan, J. Lafferty, L. Wasserman *et al.*, "High-dimensional semiparametric Gaussian copula graphical models," *The Annals of Statistics*, vol. 40, no. 4, pp. 2293–2326, 2012.
- [33] T. Zhao, H. Liu, K. Roeder, J. Lafferty, and L. Wasserman, "The huge package for high-dimensional undirected graph estimation in R," *Journal of Machine Learning Research*, vol. 13, no. Apr, pp. 1059–1062, 2012.
- [34] MSCI, "The Global Industry Classification Standard (GICS)," 2019. [Online]. Available: <https://www.msci.com/gics>.
- [35] M. J. Wainwright, *High-dimensional statistics: A non-asymptotic viewpoint*. Cambridge University Press, 2019, vol. 48.
- [36] G. Hardy, J. Littlewood, and G. Pólya, "Inequalities. Cambridge Mathematical Library Series," 1967.